A Technique for Reducing Fringe Washing Effects In L-band Aperture Synthesis Radiometry

Mark A. Fischman and A. W. England
University of Michigan, Department of Electrical Engineering and Computer Science
3124 EECS Bldg., 1301 Beal Avenue, Ann Arbor, MI 48109-2122, USA
Tel: (734) 763-4185, Fax: (734) 647-2106, e-mail: mafisch@eecs.umich.edu

Abstract—The high spatial resolution capabilities of microwave synthetic thinned array radiometry (STAR) become limited at oblique viewing angles by a phenomenon known as *fringe washing*. To alleviate this problem, we have developed a band division correlation (BDC) technique that can be implemented onto the digital back end of STAR receivers. BDC reduces the associated bandwidth in each correlator so that signal coherence is extended for large baselines in the array. In this paper, analytical and numerical solutions are presented for the point spread function of a hypothetical 27 meter L-band STAR sensor. The results show that with 4 subband channels, the BDC method improves swath edge resolution from 17.0 to 10.2 km and reduces correlation loss from 2.5 to 0.2 dB.

INTRODUCTION

Several laboratories have been developing synthetic thinned array radiometry (STAR) technology, a seminal breakthrough that will allow higher spatial resolution for Earth remote sensing instruments operating at the low end of the microwave spectrum. The European Space Agency is currently in Phase A development of a two-dimensional L-band STAR instrument for its soil moisture and ocean salinity (SMOS) mission, which should achieve between 30 and 60 km resolution. NASA centers are working on advanced sensor technology for a follow-on STAR mission with 10 km resolution that would be suitable for mesoscale hydrometeorology.

A side effect of increasing the boresight resolution of a STAR sensor is loss of image detail at swath edges. This effect, known as *fringe washing*, occurs when the time delay between a pair of received signals in the array exceeds the correlation time of the narrow band noise processed by the radiometer. For large element spacings and oblique viewing angles, the correlator output signal incurs a loss of brightness scene information at high spatial frequencies.

Ruf, *et al.* [1], have suggested splitting the receiver bandwidth into several smaller subbands before correlation and then individually transforming each visibility sample to reconstruct the image. The smaller bandwidth associated with each correlator leads to an increased correlation time. Depending on the number of band divisions, fringe washing may be reduced significantly without compromising the overall bandwidth related sensitivity of the STAR radiometer. In this paper, we an-
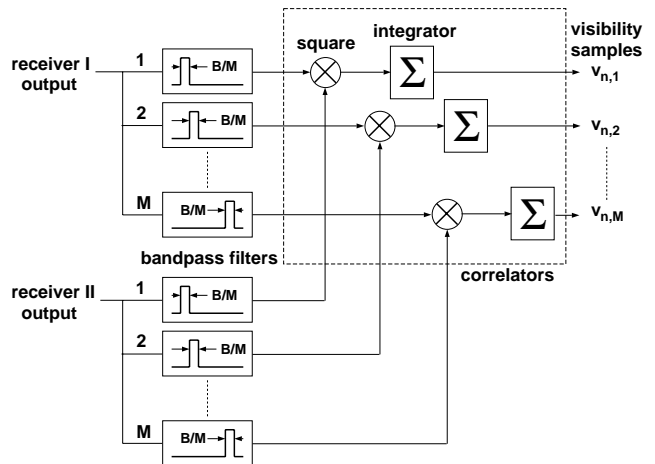

Figure 1: Schematic of a band division correlation (BDC) radiometer. The received signals, each having bandwidth *B*, are divided evenly into *M* smaller bands to reduce decorrelation effects.

alyze the efficacy of the band division correlation (BDC) concept shown in Fig. 1 for improving STAR's spatial frequency response.

A model of a one-dimensional STAR sensor in low Earth orbit will be used to compare the point spread functions for conventional correlators and for the BDC architecture. Typical design parameters for an L-band satellite are: center frequency $f_0 = 1.41$ GHz, bandwidth $B = 20$ MHz, altitude $h = 700$ km, and a field of view of $\theta = \pm 35°$. Assuming isotropic elements, a uniform array distribution, and a flat Earth across the field of view, the spatial resolution is ideally

$$\Delta x = \frac{2h}{N \cos^3 \theta}, \tag{1}$$

where N is the maximum dimension of the array in $\lambda/2$ spacings. To maintain at least 10 km resolution at the 35° border would require a STAR array size of $N = 255$, or 27 meter span. This 27 meter L-band STAR will be our reference model for evaluating the BDC architecture.

FRINGE WASHING PHENOMENON

Visibility Function

All correlation pairs in STAR generate a set of complex visibility samples for the brightness scene T_B [2]:

$$v_n = \int_{-1}^{1} T_B(\mu) \, r(n,\mu) \, e^{-j\pi n\mu} d\mu \quad \text{for } n = 0, 1, \ldots, N, \quad (2)$$

where r is the fringe washing function,

$$r(n,\mu) = \text{sinc}\left(\frac{nB\mu}{2f_0}\right), \quad (3)$$

and $\mu = \sin\theta$ is the direction sine. The impulse response for a point source centered at μ_s becomes

$$v_n = r(n, \mu_s) \, e^{-j\pi n\mu_s}. \quad (4)$$

To examine how fringe washing affects a conventional STAR's point spread function, we found inverse solutions for (2) using both Fourier transform and G-matrix approaches.

Inverse Fourier Reconstruction

If the effects of fringe washing are neglected ($r = 1$), then (2) just becomes the Fourier transform of T_B, i.e., the brightness estimate is found using the inverse Fourier series (f^{-1} reconstruction). Normalizing the response at $\mu_s = 0$ to unity, the point spread function becomes

$$\hat{T}_B(\mu) = \frac{1}{2N+1}\left[1 + 2\sum_{n=1}^{N} \text{sinc}\left(\frac{nB\mu_s}{2f_0}\right)\cos\left[\pi n(\mu - \mu_s)\right]\right]. \quad (5)$$

While the solution in (5) will show degraded resolution for large incidence angles, it is not the best estimate of the scene. A different inversion technique should be used to account for tapering of STAR's grating lobes.

Inverse G-Matrix Reconstruction

A numerical method can be used to minimize the error between the estimated and actual brightness image in STAR. The system of equations in (2) is expanded into a set of $2N+1$ real-valued visibility functions, each having an integrand that is discretized. In matrix form, this visibility vector can be written:

$$V = GT \quad (6)$$

where the rows of the G-matrix make up the STAR basis functions for the different element spacings. Because the number of points in the brightness vector T is usually oversampled above $2N+1$ to ensure that pixel size is fine enough to restore the image, the inverse solution for (6) is under-determined. For the least-squares estimate of T given by [3],

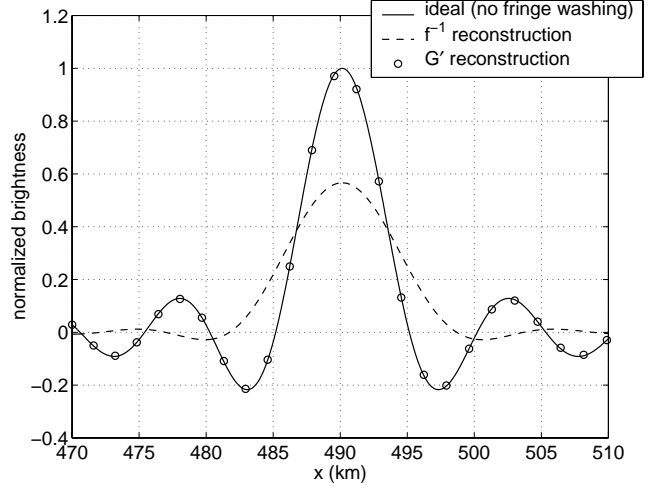$$\hat{T} = G^l V, \quad \text{where } G^l = G^t\left(GG^t\right)^{-1}, \quad (7)$$

Figure 2: Estimations of the 27 meter STAR point spread function for a source located at 35° (490 km from nadir).

we computed the elements of a G-matrix having $\sim 6N$ columns and the inverse matrix solution for the optimal point spread function. Both this G^l reconstruction and the f^{-1} reconstruction were analyzed to quantify fringe washing degradation.

Signal Degradation

Fig. 2 shows the computed point spread functions for a source located 35° from nadir. For the ideal case where there is no fringe washing, the peak response is unity, and, as predicted from (1) for the benchmark STAR radiometer, the zero-crossing beam resolution is 10.0 km. Spatial resolution for the f^{-1} reconstruction case, which includes fringe washing, is significantly lower than the ideal response. Correlation loss causes a 2.5 dB drop in the peak brightness level and a broadening of the beamwidth to 17.0 km. The pixels calculated using G^l reconstruction are also plotted with the other two curves for comparison. Here the point spread function matches the ideal response exactly. As expected, G^l reconstruction takes into account and compensates for the tapered grating lobes at large element spacings.

Although the signal response for G^l reconstruction is excellent, noise in the estimated brightness levels increases when the STAR beam is synthesized this way. The optimum solution for G^l includes inverse basis functions (columns of the matrix) whose envelops increase with incidence angle so as to compensate for the increasingly severe correlation loss. In effect, G^l reconstruction boosts a signal that has already incurred some loss, thereby boosting the inherent noise floor. For instance, in this case the system sensitivity at $\theta = 35°$ was reduced by 2.5 dB.

BAND-SLICING TECHNIQUE

Estimated Point Spread Function

The BDC receiver in Fig. 1 can potentially remove the negative effects that arise from fringe washing. Let the original receiver bandwidth B be divided equally into M smaller slices with a bank of bandpass filters. For each subband processed by a correlator, the new fringe washing function will be dilated by a factor of M:

$$r_{BDC}\left(m,n,\mu\right) = \operatorname{sinc}\left(\frac{nB\mu}{2Mf_m}\right) \qquad (8)$$

where f_m is the center frequency of each subband and $m = 1, 2, \ldots, M$ is the subband index. Equation (2) is then modified for the subband visibility samples:

$$v_{m,n} = \int_{-1}^{1} T_B\left(\mu\right) r_{BDC}\left(m,n,\mu\right) \exp\left(-j\pi n f_m \mu / f_0\right) d\mu. \qquad (9)$$

The normalized brightness estimate is found by taking the impulse response in (9) and transforming these visibilities with an inverse Fourier series:

$$\hat{T}_B\left(\mu\right) = \frac{1}{2N+1} \times \qquad (10)$$

$$\left[1 + \frac{2}{M} \sum_{m=1}^{M} \sum_{n=1}^{N} \operatorname{sinc}\left(\frac{nB\mu_s}{2Mf_m}\right) \cos\left[\pi n f_m \left(\mu - \mu_s\right) / f_0\right]\right].$$

The reconstructed image can be calculated for the benchmark STAR over a range of band divisions to assess the improvement in spatial resolution.

Numerical Results

The BDC STAR point spread function in (10) was computed over the field of view for several different values of M. Fig. 3 shows a plot of the resulting spatial resolution and peak correlation loss compared to the ideal case. With just 2 subbands, there is already a marked improvement in resolution from 17.0 km to 11.0 km at $35°$ incidence; with $M = 4$, the resolution approaches a nearly ideal value of 10.2 km. Also the correlation loss at the peak of the impulse response is reduced greatly with only a few band divisions. Compared to a conventional STAR with a 2.5 dB correlation loss, the BDC loss figure can be improved to 0.6 dB (for $M = 2$) or as low as 0.2 dB (for $M = 4$).

The STAR sensor considered here quickly converges to the "no fringe washing" case with a relatively small number of subband correlators. This implies that noise in high spatial frequency visibility samples can be reduced more effectively in a STAR sensor that employs BDC than in a sensor that used conventional correlators and G^I post-processing. The BDC concept is also suited for present day STAR systems where the received brightness signals are digitized at IF or RF frequencies to transfer signal processing complexity to the digital domain. Given the availability of DSP devices that run at 10^9 operations/second, it is realistic to develop L-band BDC radiometers having up to 4 frequency selective bands.
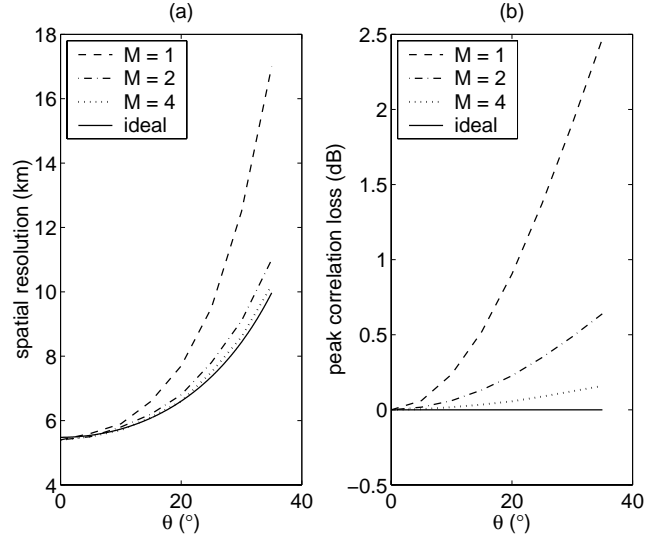

Figure 3: (a) Spatial resolution vs. incidence angle for a conventional STAR ($M = 1$), for a BDC instrument with $M = 2$ and 4 divisions, and for the ideal case. (b) Peak level correlation loss for the above cases.

CONCLUSION

The fringe washing problem encountered in high resolution L-band STAR radiometry can be alleviated by using a novel band division correlation processor. An analysis of a 27 meter BDC STAR sensor has shown that, with 4 channels of subband processing, this technique will virtually eliminate decorrelation effects that would normally add noise to high spatial frequency brightness signals.

REFERENCES

[1] C. S. Ruf, C. T. Swift, A. B. Tanner, and D. M. Le Vine, "Interferometric synthetic aperture microwave radiometry for the remote sensing of the earth," *IEEE Trans. Geosci. Remote Sensing*, vol. 26, pp. 597–611, Sept. 1988.

[2] B. Laursen and N. Skou, "Synthetic aperture radiometry evaluated by a two-channel demonstration model," *IEEE Trans. Geosci. Remote Sensing*, vol. 36, pp. 822–832, May 1998.

[3] A. B. Tanner and C. T. Swift, "Calibration of a synthetic aperture radiometer," *IEEE Trans. Geosci. Remote Sensing*, vol. 31, pp. 257–267, Jan. 1993.